Inverting equation A3.14

Convolution Theorem

$$\mathcal{L}^{-1}\, g_1(s).g_2(s) = \int_0^t g_1(\tau).g_2(t-\tau).d\tau \qquad \text{A3.15}$$

$$g_1(s) = \left(\frac{a}{a+s}\right)^N , \qquad g_2(s) = \frac{1}{s}$$

$$\therefore C_N(t) = a^N \int_0^t 1.\frac{\tau^{N-1}}{(N-1)!}.e^{-a\tau}\, d\tau . \qquad \text{A3.16}$$

$$= a^N \left[e^{-a\tau} \sum_{r=0}^{N-1} \frac{(-1)^r \quad \tau^{(N-1-r)}}{(N-1-r)!\ (-a)^{r+1}} \right]_0^t \qquad \text{A3.17}$$

NB. $$a^N . \sum_{r=0}^{N-1} \frac{(-1)^r}{(-a)^{r+1}} = - \sum_{r=0}^{N-1} a^{N-1-r}$$

$$\therefore C_N(t) = -e^{-at}. \sum_{r=0}^{N-1} \frac{(at)^{N-1-r}}{(N-1-r)!} + e^0 . \sum_{r=0}^{N-1} \frac{0^{N-1-r}}{(N-1-r)!}$$

A3.18

NB. @ $r = N-1$ The second term becomes :

$$\frac{0^0}{0!} = 1$$

$$\therefore \; C_N(t) = 1 - e^{-at} \cdot \sum_{r=0}^{N-1} \frac{(at)^{N-1-r}}{(N-1-r)!} \qquad \text{—— A3.19}$$

Setting N = 1

$$C_1(t) = 1 - e^{(-ut/V_T)} \qquad \text{—— A3.20}$$

Setting N = 2

$$C_2(t) = 1 - e^{(-2ut/V_T)} \cdot (2ut/V_T + 1) \qquad \text{—— A3.21}$$

Which are consistant with the individual solutions to a single tank and two tanks respectively.

A3.3 Response to a Step-change through a Series of Uniform Stirred Tanks With Associated 'Dead-spaces'

In section(7.4.3) it is shown that a series of of uniform stirred tanks with associated 'dead-spaces' may be approxiamated by a simple series of uniform stirred tanks with a single 'dead-space'. The mathematial analysis of the simple series of stirred tanks may there fore be extended to account for the attached 'dead-space'. From figure(7.9) the last tank in the simple series and the 'dead-space' are shown in figure (A3.4) below.

Figure (A3.4) Flow arrangement for Levichs' model.

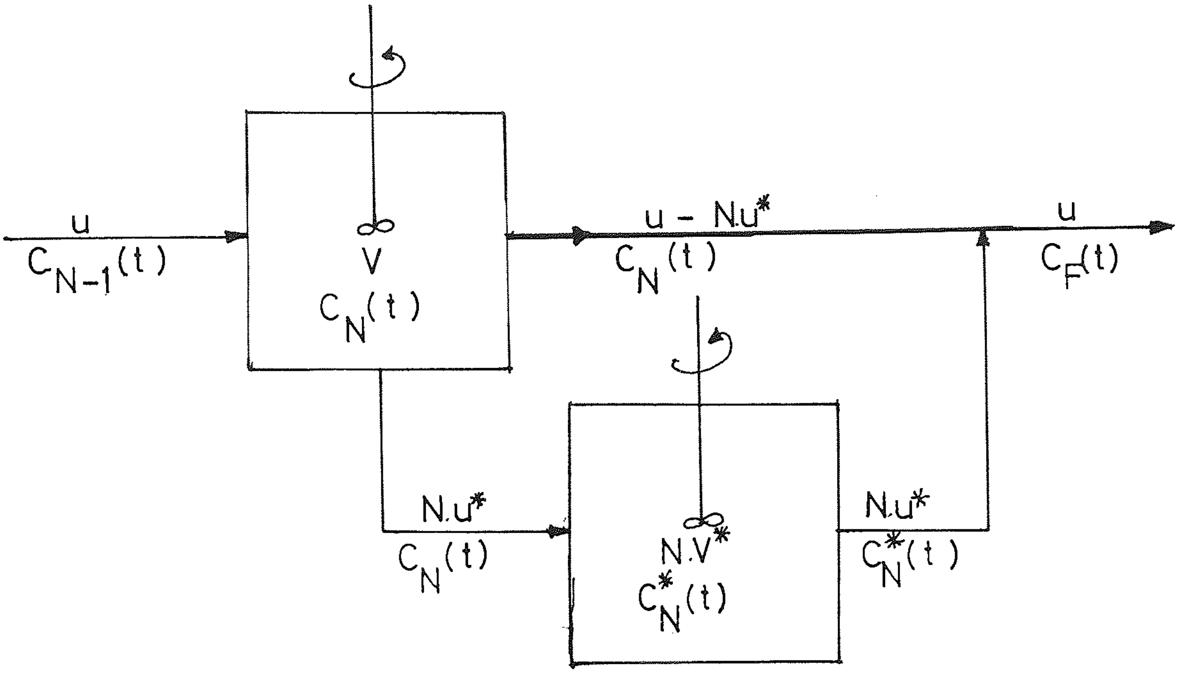

where $C_F(t)$ —— Final outlet concentration @ time 't'.

$C_N^*(t)$ —— Outlet concentration from 'dead-space' @ time 't'.

V —— Volume of a single stirred tank (L^3)

$N.V^*$ —— Total volume of 'dead-space' (L^3)

$N.u^*$ —— Total flow-rate into the 'dead-space' (L^3/θ)

Combining the two outlet streams to give $C_F(t)$

$$C_F(t) = (N.u^*.C_N^*(t) + (u - Nu^*).C_N(t))/u \qquad \text{A3.22}$$

Dynamic mass balance across the 'dead-space'

$$Nu^* C_N(t) = Nu^* C_N^*(t) + NV^* \frac{dC_N^*(t)}{dt} \qquad \text{A3.23}$$

Taking Laplace transforms (neglecting perturbation variable notation) and rearranging:

$$C_N(s) = C_N^*(s) + \frac{V^*}{u^*}(s.C_N^*(s) + 0) \qquad \text{A3.24}$$

$$b = \frac{u^*}{V^*}$$

$$\therefore C_N^*(s) = \left(\frac{b}{b+s}\right) . C_N(s) \qquad \text{A3.25}$$

$C_N(s)$ is given by the response to a step-change through a simple series of uniform stirred tanks, as already described.

$$\therefore C_N(s) = \frac{1}{s} . \left(\frac{a}{a+s}\right)^N . \left(\frac{b}{b+s}\right) \qquad \text{A3.26}$$

In this case, $a = \frac{u}{V}$

Inverting equation A3.26

Convolution Theorem

$$\mathcal{L}^{-1} g_1(s).g_2(s) = \int_0^t g_1(\tau).g_2(t-\tau).d\tau$$

Let $g_1(s) = \frac{1}{s}\left(\frac{a}{a+s}\right)^N$, $g_2(s) = \left(\frac{b}{b+s}\right)$

$$\therefore C_N^*(t) = \int_0^t \left(1 - e^{-a\tau} . \sum_{r=0}^{N-1} \frac{(a\tau)^{N-1-r}}{(N-1-r)!}\right)\left(be^{-b(t-\tau)}\right).d\tau$$

$$\text{A3.27}$$

$$\therefore C_N^*(t) = \int_0^t \left(be^{-b(t-\tau)} - e^{\tau(b-a)} e^{-bt} b \sum_{r=0}^{N-1} \frac{(a\tau)^{N-1-r}}{(N-1-r)!} \right) . d\tau$$

Separately considering the term, $be^{-b(t-\tau)}$

$$\int_0^t be^{-b(t-\tau)} d\tau = \left[-e^{-(b-\tau)} \right]_0^t \quad \text{——— A3.28}$$

$$= 1 - e^{-bt} \quad \text{——— A3.29}$$

Considering each term of the summation separately, setting $p = N-1-r$

$$\frac{be^{-bt}}{p!} \int_0^t e^{\tau(b-a)} (a\tau).d\tau = a^p . be^{-bt} \left[e^{\tau(b-a)} \sum_{q=0}^{p} \frac{(-1)^q \tau^{p-q}}{(p-q)!(b-a)^{q+1}} \right]_0^t$$

——— A3.30

Inserting the limits and combining all the terms, taking $0^0 = 1$

$$C_N^*(t) = 1 - e^{-bt} - \sum_{r=0}^{N-1} \left(\left(a^p . be^{-at} \sum_{q=0}^{p} \frac{(-1)^p t^{p-q}}{(p-q)!(b-a)^{q+1}} \right) \right.$$

$$\left. - \left(\frac{(-1)^p a^p be^{-bt}}{(b-a)^{p+1}} \right) \right) \quad \text{——— A3.31}$$

NB. $$\frac{(-1)^p}{(b-a)^{p+1}} = \frac{-1}{(a-b)^{p+1}}$$

$$\therefore C_N^*(t) = 1 - e^{-bt} + b \sum_{r=0}^{N-1} a^p \left(e^{-at} \sum_{q=0}^{p} \frac{t^{p-q}}{(p-q)!\,(a-b)^{q+1}} - \frac{e^{-bt}}{(a-b)^{q+1}} \right) \qquad \text{A3.32}$$

NB. A different selection of the order in which the Convolution theorem is applied will yield a mathematically identical solution but of quite different appearance.

Setting N = 1

$$\therefore p = 0,\ r = 0,\ q = 0$$

$$C_1^*(t) = 1 - \frac{b e^{-at}}{(b-a)} - \frac{a e^{-bt}}{(a-b)} \qquad \text{A3.33}$$

which is consistent with the solution for the response to a step-change through two non-uniform tanks in series.

For the purpose of computer applications the summations must range from a finite start, hence the following substitutions are made:

$$r = M - 1, \quad q = L - 1, \quad NM = N - M + 1$$

and the limits are increased by 1

$$\therefore C_N^*(t) = 1 - e^{-bt} + b \sum_{M=1}^{N} a^{N-M} \left(e^{-at} \sum_{L=1}^{NM} \frac{t^{N+1-M-L}}{(N+1-M-L)!\,(a-b)^{L}} - \frac{e^{-bt}}{(a-b)^{N-M+1}} \right) \qquad \text{A3.34}$$

If $a = b$, then there is no solution to equation A3.32, since the term $(a - b)$ appears in the denominator. Then considering equation A3.26 again, setting $b = a$:-

$$C_N^*(s) = \frac{1}{s} \cdot \left(\frac{a}{a+s}\right)^N \cdot \left(\frac{a}{a+s}\right)$$

$$= \frac{1}{s} \cdot \left(\frac{a}{a+s}\right)^{N+1} \equiv C_{N+1}^*(s)$$

$$\therefore \quad C_F(t) = \frac{(u - N.u^*).C_N(t) + N.u^* C_{N+1}(t)}{u} \qquad \text{——— A3.35}$$

As shown in figure (7.5), while 'N' is relatively high, 6 ~ 8 say, $C_N(t) \simeq C_{N+1}(t)$; hence the solution to $C_F(t)$ approximates to a simple series of stirred tanks and may thus give rise to a straight line plot on log:normal probability scales.

A3.4. Stirred Tank Model with Associated 'Dead space' with Re-entry Considered.

Considering the material balance over the 'dead space' from figure (7.10) as shown below in figure A3.5.

Figure A3.5 'Dead space' with re-entry considered.

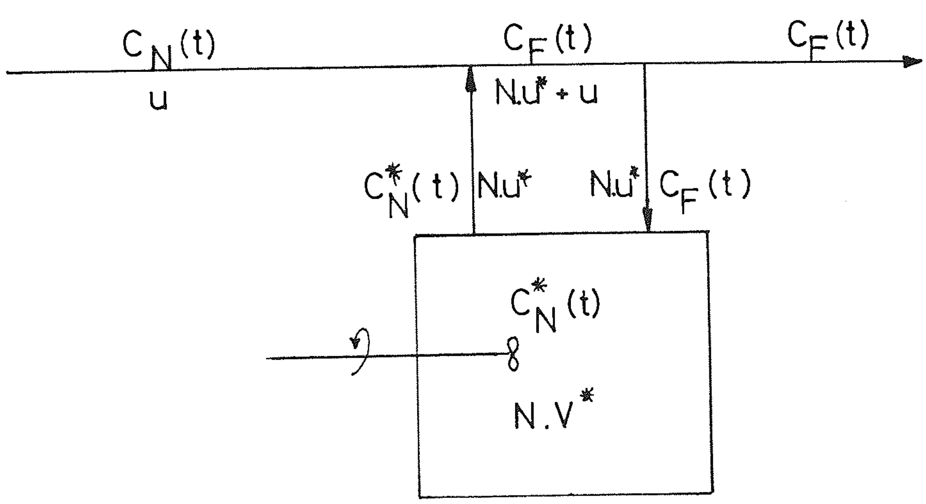

Material Balance for $C_F(t)$

$$C_F(t) = \frac{N u^* C_N^*(t) + u . C_N(t)}{(N.u^* + u)} \qquad \text{A3.36}$$

Rate of accumulation of tracer in 'dead space'

$$\frac{dC_N(t)}{dt} = \left(\frac{\not{N}.u^*}{\not{N}.V^*}\right) \cdot \left(C_F(t) - C_N^*(t)\right)$$

$$= \left(\frac{u^*}{V^*}\right) \cdot \left(\frac{N.u^* C_N^*(t) - u C_N(t)}{(N.u^* + u)} - C_N^*(t)\right)$$

$$= \left(\frac{u^*}{V^*}\right)\left(\frac{u}{Nu^* + u}\right)\left(C_N(t) - C_N^*(t)\right) \qquad \text{A3.37}$$

The term $\left(\frac{u^*}{V^*}\right)\left(\frac{u}{Nu^* + u}\right)$ may be regarded as a mass transfer coefficient multiplied by the 'wetted surface area'. This compares to $\frac{u^*}{V^*}$ in the case when no re-entry is considered. Both models require that u^* is relatively small compared to u; they may then be expected to yield similar values for the 'mass transfer coefficient', while different values of $\frac{u^*}{V^*}$ may be anticipated.

APPENDIX(4)

Computer Flow Diagram for the Optimization of the Hydraulic Model Parameters

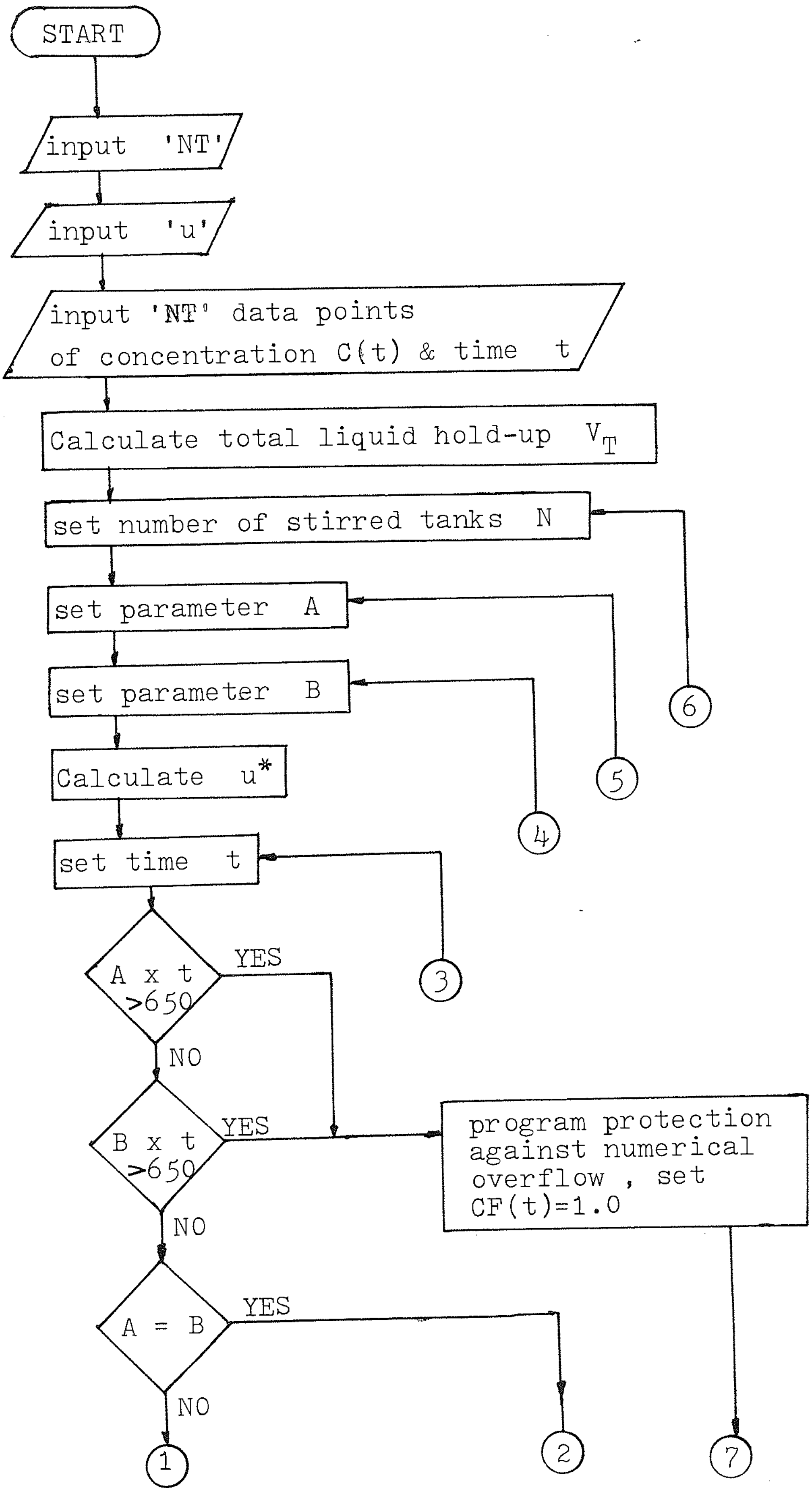

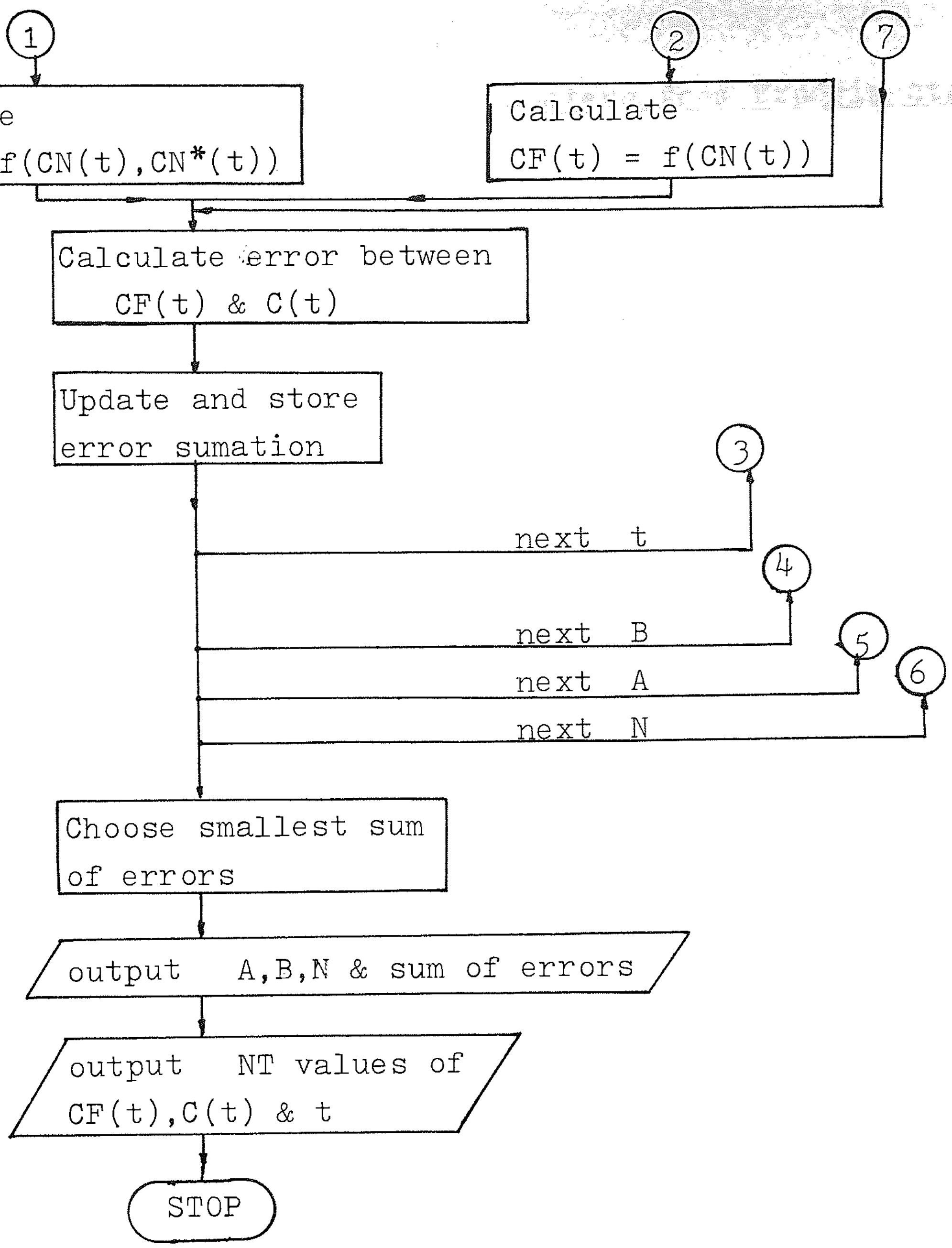
1
2
7
Calculate
CF(t) = f(CN(t),CN*(t))
Calculate
CF(t) = f(CN(t))
Calculate error between
CF(t) & C(t)
Update and store
error sumation
3
next t
4
next B
5
next A
6
next N
Choose smallest sum
of errors
output A,B,N & sum of errors
output NT values of
CF(t),C(t) & t
STOP

APPENDIX (5)

Appraisal of Kinetic and Hydraulic Parameters from Experiments on the Biopac 50 Rig.

Table (A5.1) shows the inlet and outlet glucose concentrations that were measured immediately prior to each tracer experiment on the Biopac 50 rig.

Table (A5.1) Glucose Concentrations on the Biopac 50 Rig Prior to Tracer Experiments.

Flow Rate $cm^3 s^{-1}$	Glucose Concentrations mg/l	
	Inlet	Outlet
0.75	515	392
1.30	513	420
1.95	537	450
2.60	483	421
3.90	491	450
5.15	549	515

Assuming a constant wetted surface area and plug-flow, simple mass balance using bulk 0', ½' and 1st order kinetics may be used to evaluate the respective combined constants. The differential mass balance for a surface area-dependent reaction with plug-flow is given by equation (A5.1): see section (6.3).

$$\int_{C_{out}}^{C_{in}} \frac{dC}{(-r_a)} = \frac{A}{u} \qquad \text{A5.1}$$

where A ———— total wetted surface area within the systems (L) or specific wetted surface area x volume of system

C ———— concentration of rate-limiting substrate (ML^{-3})

u ———— volumetric flow rate ($L^3\theta^{-1}$)

$(-r_a)$ ———— rate of limiting substrate removal per unit wetted surface area ($M\theta^{-1}L^{-2}$).

0' order Case.

$$(-r_a) = k_o \bar{F} \qquad 2.4$$

where k_o ———— intrinsic zero order rate constant ($M\theta^{-1}L^{-3}$)

$\bar{F}$ ———— mean microbial film thickness (L)

½' order Case.

$$(-r_a) = \sqrt{2 k_o D C} \qquad 2.5$$

where D ———— apparent diffusivity of rate-limiting substrate through microbial film ($L^2\theta^{-1}$).

1st order Case.

$$(-r_a) = \sqrt{\frac{k_o D}{k^*}}\, C \qquad 2.6$$

where k^* ———— constant (ML^{-3}).

On substitution of these three rate expressions into equation (A5.1), the integrated mass balances can be rearranged to give the combined constants, as follows:

0' order Case. (assuming constant $\bar{F}$).

$$k_o A . \bar{F} = u(C_{in} - C_{out}) \qquad A5.2$$

½' order Case.

$$A\sqrt{\frac{k_o D}{2}} = u(\sqrt{C_{in}} - \sqrt{C_{out}}) \qquad A5.3$$

1st order Case.

$$A\sqrt{\frac{k_o D}{k^*}} = u . \ln\left(\frac{C_{in}}{C_{out}}\right) \qquad A5.4$$

The values of the three grouped constants, represented by the left hand sides of the equations A5.2, 5.3&5.4 are shown plotted against the flow rate, u , in figures A5.1a,b&c and are also presented in Table (A5.2) at the end of this

Figure (A51a,b&c) The Combined Constants .vs. Flow-rate Assuming Plug Flow & Constant Wetted Area

(a) Zero Order Case (Assuming Constant $\bar{F}$)

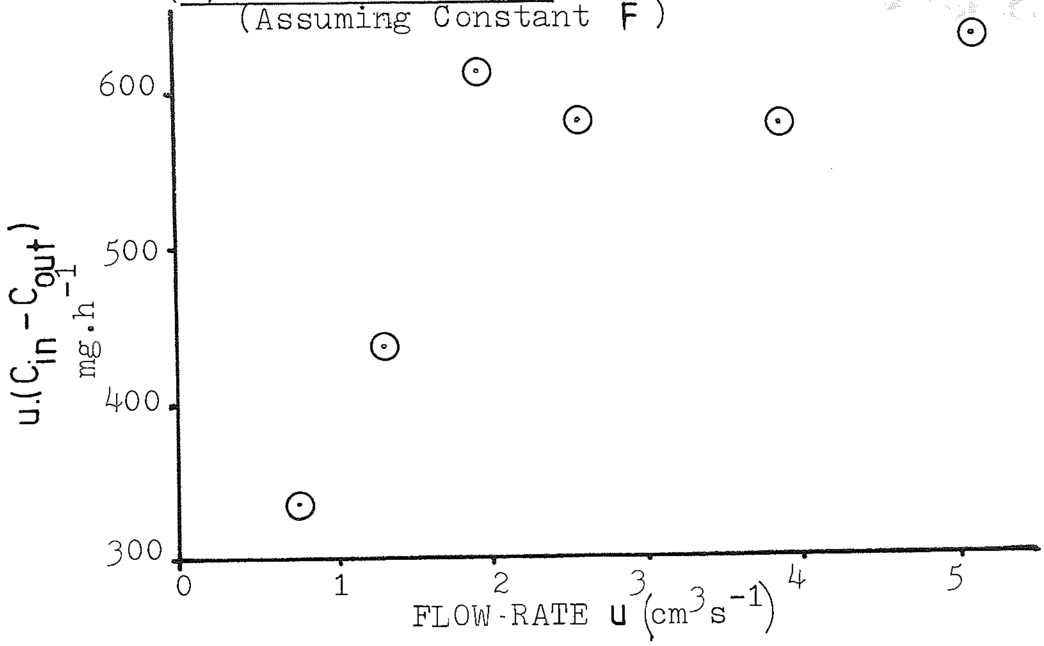

(b) '½' Order Case

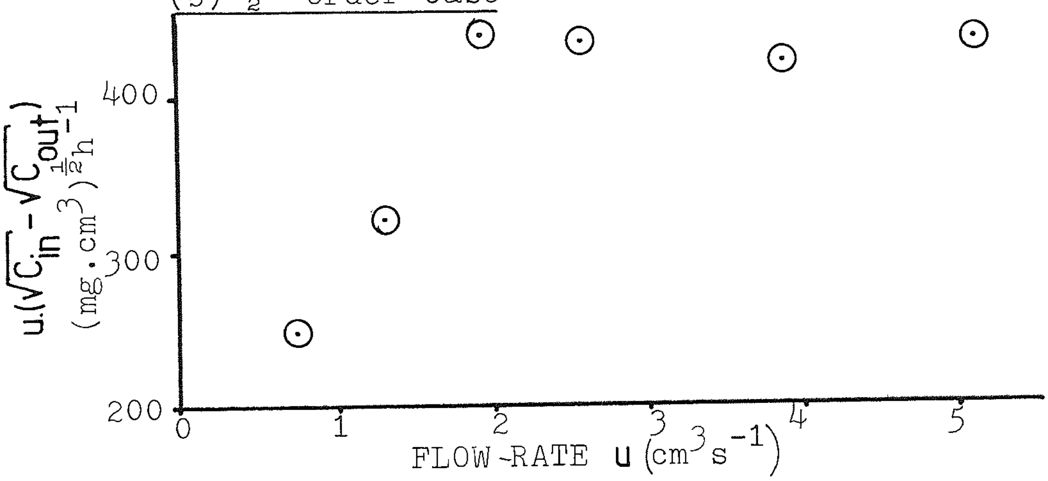

(c) 1st. Order Case

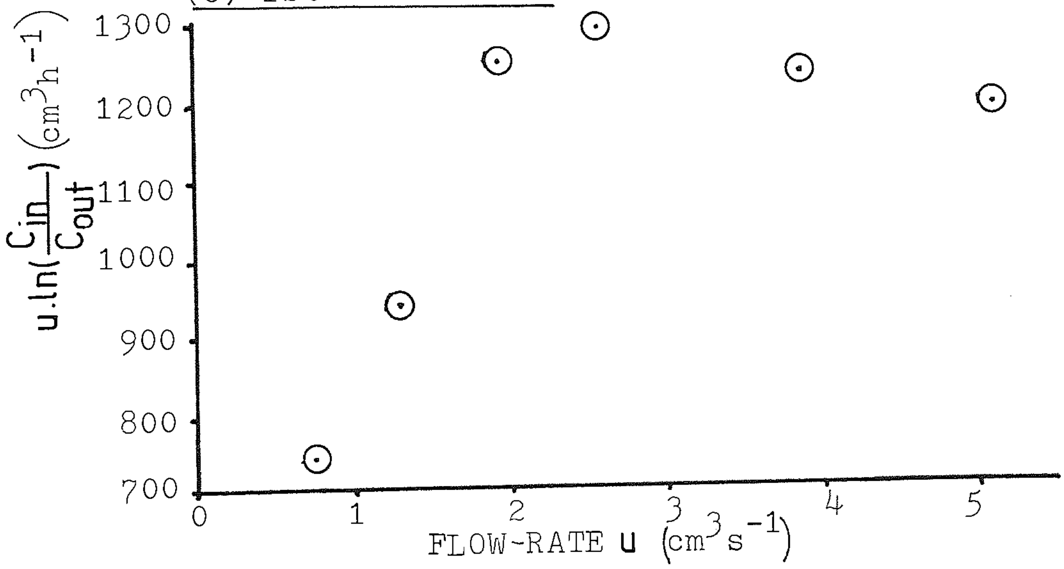

appendix. It is clear from Figures A5.1a,b&c that none of these simplified models adequately describes filter performance, since the grouped constants are all functions of the flow rate, u.

The total wetted surface area, A, and the degree of liquid mixing, which are quantified in Chapter 8, may be taken into account with the three kinetic models as shown below. The specific wetted surface area is taken to be a function of irrigation rate according to Figure (8.4) and the liquid mixing is expressed in terms of the number of stirred tanks, N, as given in Table (8.3). In the zero-order case, account may also be taken of variations in the microbial film thickness, $\bar{F}$, using the total liquid hold-up, V_T, and the liquid film thickness, δ, as given in Table (8.3).

<u>0' order Case.</u>

As stated in Section (7.1), liquid mixing is of no consequence with zero-order kinetics; hence, the zero-order rate constant, k_o, is given by

$$k_o = \frac{u}{\bar{F} A} (C_{in} - C_{out}) \quad \text{A5.5}$$

The mean microbial film thickness, $\bar{F}$, may be estimated from

$$\bar{F} = \frac{(\text{volume of microbial film})}{(\text{area of packing covered by film})} \quad \text{A5.6}$$

where

volume of microbial film = (total liquid hold-up) - (volume of flowing liquid)

and

volume of flowing liquid = (wetted surface area) x (liquid film thickness)

Since all the available surface area of packing was covered with microbial film:

$$\begin{pmatrix}\text{area of packing}\\ \text{covered with film}\end{pmatrix} = \begin{pmatrix}\text{specific surface}\\ \text{area of Biopac 50}\end{pmatrix} \times \begin{pmatrix}\text{volume of}\\ \text{packing}\end{pmatrix}$$

$$= \quad 1.26 \frac{cm^2}{cm^3} \quad x \quad 1784 \; cm^3$$

$$\overline{F} = \frac{V_T - (A.\delta)}{2248 \; cm^2} \qquad \text{A5.7}$$

Calculated values of k_o are plotted against the flow rate, u, in Figure A5.2a. The values of k_o, $\overline{F}$, and A are shown in Table A5.2 along with the corresponding values of V_T and δ, which are reproduced from Table 8.3.

$\frac{1}{2}$' order Case.

The material balance over a single theoretical stirred tank with $\frac{1}{2}$' order surface area- dependent kinetics is given by

$$C_{in} = C_{out} + \frac{A}{u} \sqrt{2 k_o D C_{out}} \qquad \text{A5.8}$$

Therefore, the material balance over the nth tank in a series of N tanks is given by:-

$$C_{n-1} = C_n + \frac{A}{u} \sqrt{2 k_o D C_n} \qquad \text{A5.9}$$

For given values of C_{in}, C_{out}, total wetted surface area A, and number of theoretical stirred tanks, N, the combined term $\sqrt{2 k_o D}$ is most conveniently found by an iterative calculation. The values of $\sqrt{2 k_o D}$ obtained in this way are plotted against the flow-rate, u, in Figure A5.2b. The values of $\sqrt{2 k_o D}$ and N are also listed in Table A5.2 .

1st order Case.

The material balance over a single theoretical stirred tank with 1st order surface area-dependent kinetics is given by

$$C_{in} = C_{out} + \frac{A}{u} \sqrt{\frac{k_o D}{k^*}} \; C_{out} \qquad \text{A5.10}$$

Therefore, the material balance over the nth tank in a series

Figure(A5.2a,b&c) The Combined Constants .vs. Flow-rate With the Hydraulic Parameters Accounted For

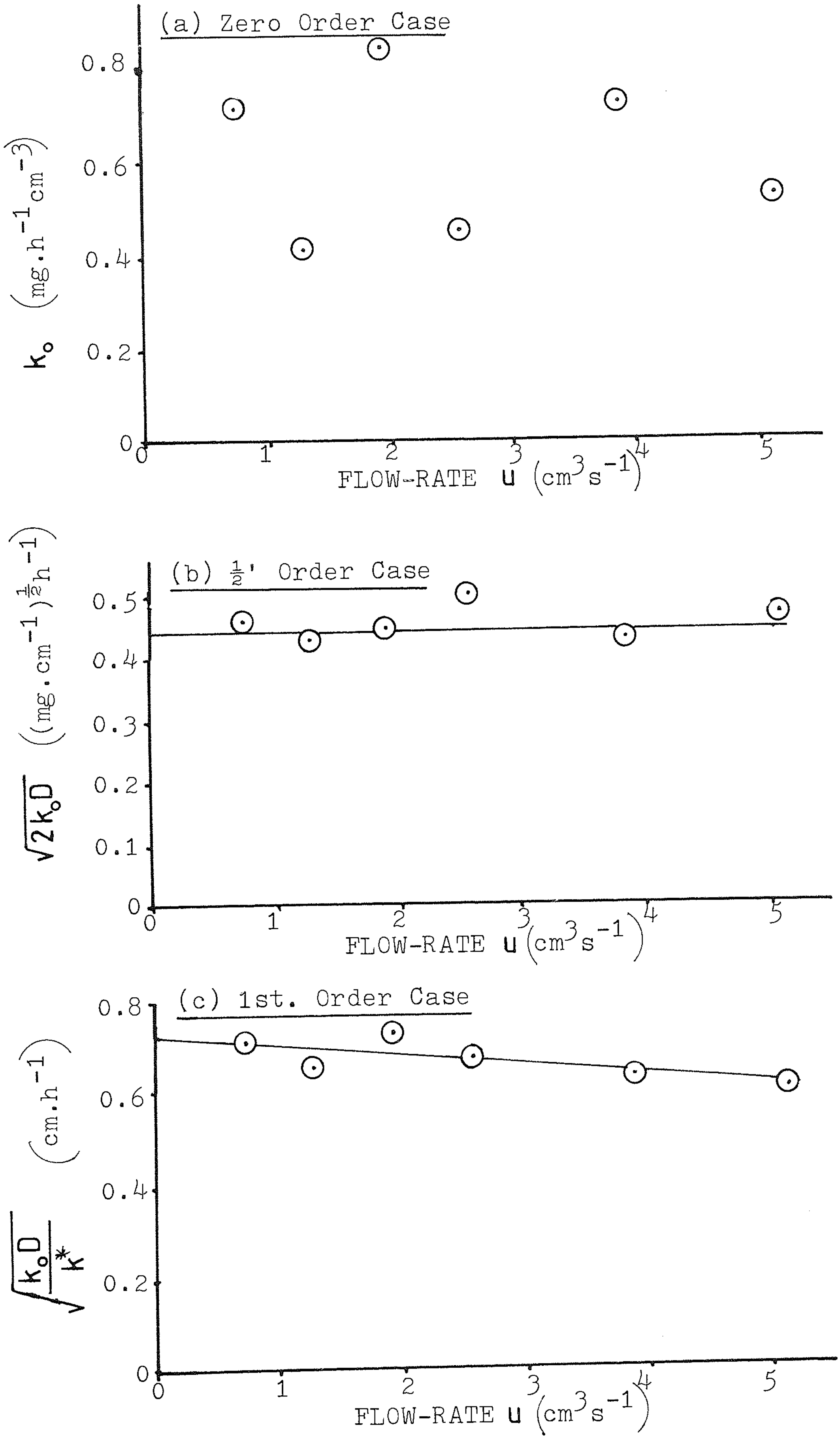

of N tanks is:

$$C_{n-1} = C_n \left[1 + \frac{A}{uN}\sqrt{\frac{k_o D}{k^*}}\right] \qquad \text{A5.11}$$

The balance over the series of N tanks is, consequently:

$$C_{in} = C_{out}\left[1 + \frac{A}{uN}\sqrt{\frac{k_o D}{k^*}}\right]^N \qquad \text{A5.12}$$

Rearranging:

$$\sqrt{\frac{k_o D}{k^*}} = \frac{uN}{A}\left[\left(\frac{C_{in}}{C_{out}}\right)^{(1/N)} - 1\right] \qquad \text{A5.13}$$

The calculated values of the combined term, $\sqrt{\frac{k_o D}{k^*}}$ are plotted against the flow-rate, u, in Figure A5.2c and are listed in Table A5.2 .

Figure A5.2a shows that with due account being taken of the wetted surface area and microbial film thickness variations the zero order kinetics are not applicable. Figures A5.2a&b show that with due account being taken of wetted surface area and liquid mixing variations either $\frac{1}{2}$' or 1st order kinetics could be applied. This apparent choice is due to the experimental errors and small concentration changes associated with such a small test system of this kind. The 1st order case is however seen to give a negative slope in Figure A5.2c which could indicate that 1st order kinetics are inappropriate, given that the hydraulic parameters are correctly defined. The $\frac{1}{2}$' order kinetics are confirmed in Chapter 6 using the inclined plane, hence Figure A5.2b confirms the hydraulic parameters.

A Comparison of Kinetic Parameters Evaluated from Experiments on the Biopac 50 Rig and the Inclined Plane - the Effect of the Temperature Correction.

The $\frac{1}{2}$' order kinetic parameters obtained from experiments on the inclined plane and the Biopac 50 experiments cannot be compared directly since the ambient temperatures

Table A5.2 Summary of Kinetic and Hydraulic Parameters Obtained From Biopac 50 Experiments.

u $cm^3.s^{-1}$	$u(C_{in}-C_{out})$ $mg.h^{-1}$	$u(\sqrt{C_{in}}-\sqrt{C_{out}})$ $(mg.cm^3)^{\frac{1}{2}}h^{-1}$	$u.\ln(\frac{C_{in}}{C_{out}})$ $cm^3.h^{-1}$	A cm^2	N	V_T cm^3	δ mm	$\bar{F}$ mm	k_o $mg.h^{-1}.cm^{-3}$	$\sqrt{2k_oD}$ $(mg.cm^{-1})^{\frac{1}{2}}h^{-1}$	$\sqrt{\frac{k_o.D}{k^*}}$ $cm.h^{-1}$
0.75	332	247	737	1100	2	1025	0.76	4.19	0.720	0.460	0.718
1.30	435	319	936	1525	2	1740	1,18	6.94	0.411	0.423	0.646
1.95	611	435	1241	1782	2	1052	0.85	4.01	0.855	0.446	0.728
2.60	580	432	1286	1952	4	1628	0.87	6.49	0.458	0.502	0.670
3.90	576	420	1224	2028	1	1049	0.84	3.91	0.726	0.429	0.631
5.15	630	432	1185	2028	1	1478	0.71	5.93	0.524	0.467	0.604
							Mean		0.616	0.455	0.666
							Std. dev^{n}.		±29%	±6.3%	±7.4%

were different in each case. They can, however, be compared using published temperature corrections for high-rate filters and other biological reactors. The general form of a temperature correction is given by equation 2.8, and, as is discussed in section 2.5 , the published correction factors apply to the bulk rate constants and not the intrinsic constants. Hence, with ½' order kinetics the published temperature corrections should be applied to the term $\sqrt{2\,k_0 D}$. Since the diffusivity, D , is expected to be independent of small temperature changes, the effect on the intrinsic rate constant, k_0 , may be readily evaluated.

The bulk kinetic temperature correction for high-rate biological filters, based on data from several workers and included in the literature review of Roberts (see Chapter 2) is given by:

$$\text{temperature correction between temperatures } T_B \text{ and } T\,(^\circ C) = 1.041^{(T-T_B)}$$

The Biopac 50 experiments were conducted at 15°C and the inclined plane experiments were conducted at 22°C. Therefore, as a first approximation,

$$\left(\sqrt{2k_0D}\right)_{22^\circ C} = \left(\sqrt{2k_0D}\right)_{15^\circ C} \times 1{\cdot}041^{(22-15)}$$

$$= 0.455 \times 1.325$$

$$= 0.603 \ (\text{mgcm}^{-1})^{\frac{1}{2}}\text{h}^{-1}$$

Taking a constant diffusivity, D, at an intermediate glucose concentration from Table 6.4 i.e. $D = 2.07 \times 10^{-5}\text{cm}^2\text{s}^{-1}$,

$$k_0 \ (\text{Biopac @ } 22^\circ C) = \frac{(0.603)^2 \text{mgcm}^{-1}\text{h}^{-2}}{2 \times 2.07 \times 10^{-5}\text{cm}^2\text{s}^{-1}} \times \frac{1\text{h}}{3600\text{s}}$$

$$= 2.4 \ \text{mg.cm}^{-3}\text{h}^{-1}$$

This value compares favourably with the value obtained from the inclined plane using concentration measurements

(2.5 $mgcm^{-3}h^{-1}$), but is lower than the values obtained using microbial film thickness measurements (3.6 $mgcm^{-3}h^{-1}$). It should, however, be noted that the Biopac 50 experiments were not maintained at a constant temperature hence the 7°C temperature difference quoted is approximate and the temperature correction is not necessarily specific to this system.

APPENDIX (6)

A6.1 Summary of the Glucose Analysis.

The glucose concentrations were determined by the colourimetric method of Dubias et al. for sugars and related compounds. This method is suitable for sugars both in aqueous solution and bound within microbial cells in the concentration range 20 - 100mg/l. The essential features are summarised below for the rapid, accurate determination of dissolved glucose; a typical calibration plot is shown in Figure A6.1.

1) All glassware should be clean and oven dried; solvent drying should be avoided.
2) The liquid samples should be filtered to remove any suspended micro-organisms/solids.
3) The samples should be diluted to within the specified concentration range, preferably towards the top of the range, to maintain a high accuracy. When small samples are being handled, the dilutions may be best carried out by weighing the sample and the quantity of water added.
4) $1cm^3$ of diluted sample is transfered to a large bore boiling tube, preferably using an autopipette.
5) $1cm^3$ of Analar 5% phenol solution by weight is added and mixed.
6) $5cm^3$ of Analar concentrated sulphuric acid is added rapidly. It is essential that the acid is added rapidly to achieve the highly exothermic reaction and avoid the formation of a double layer; hence the need for large bore boiling tubes. An automatic dispenser is essential for the safe, rapid and accurate metering of the acid.
7) The boiling tubes are tilted and rotated to pick up any liquid splashed up the sides of the tubes. They are then covered and left to stand for half an hour for the colour

Figure A6.1 Typical Calibration of the SP 1800 Spectrophotometer for Glucose Analysis

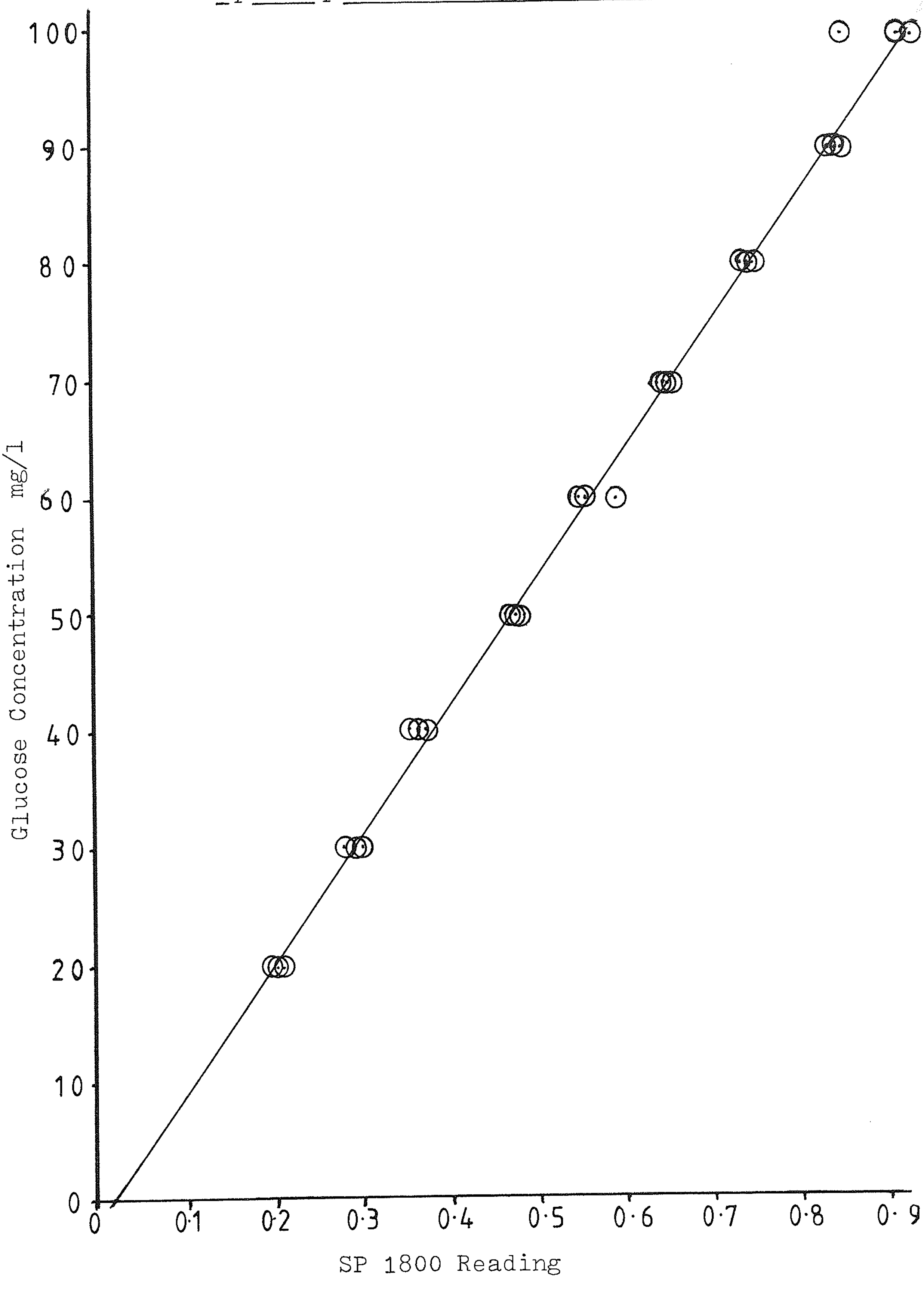

to fully develop.

8) The light absorption is measured at a wavelength of 490nm on a suitably calibrated spectrophotometer. The colour intensity may be affected by the presence of salts and the calibration should account for this.

9) The exothermic reaction can occasionally fail, hence each sample should be treated in triplicate.

A6.2 Microbial Film Thickness Measurements.

Locating the Film Thickness Measurements.

As described in Chapter 3, the inclined plane was divided into eight sections of equal length. It was desired to take a number of microbial film thickness measurements in each of these eight sections at preset positions, to eliminate any bias. In addition, it was considered desirable that the measurements be evenly spaced, but randomly located, over each section. To achieve this, each section was divided into four smaller subsections of equal length. Each subsection was divided into a grid of 0.5cm squares. Each grid square was allocated a number (grid reference). Finally, to achieve a representative film thickness analysis over each section of the inclined plane, a number of film thickness measurements were taken in each of the subsections at grid references determined by random numbers.

Number of Film Thickness Measurements.

The minimum number of measurements that would give a representative analysis of the microbial film thickness in each section of the inclined plane was determined by the method described below.

Film thickness measurements were taken on a section of the inclined plane until both the arithmetic mean and the standard deviation became stable; this was achieved after eight measurements. A further eight measurements were taken and the means,standard deviations and the distribution of the measurements were compared for the two sets of eight measurements and the total sixteen measurements: all compared favourably. A particularly harsh case was deliberately chosen whereby approximately half of the microbial film had previously broken away. Ten measurements were then considered to be capable of giving a representative analysis of the film thickness in all cases.

A6.3 Use and Calibration of the Specific Bromide Ion Electrode.

An Orion specific bromide ion electrode (model 94 - 35A) connected to a Corning pH/mV meter combined with a Fluke digital voltmeter was used to measure the bromide ion concentrations in the tracer studies decribed in Chapter 7. The combination of the two instruments achieved an order of magnitude improvement in the accuracy in which the electrode output could be measured; in addition, the stability of the mV readings was also improved. The response time of the electrode to changes in concentration was found to be unpredictable; hence the electrode could not be used to monitor tracer concentrations <u>in situ</u>. It was therefore necessary to collect small batch samples during the tracer experiments for subsequent analysis. The electrode was found to give accurate results when correctly maintained. If, however, the tip of the electrode became slightly soiled, gross inaccuracies were encountered. Frequent cleaning with the cleaning agents supplied with the electrode was found to eliminate this problem. In some instances, cleaning was necessary between every third or fourth sample. It was found necessary to recalibrate the electrode on each occasion the instruments were set up; a typical calibration is shown in Figure A6.2. In calibrating the electrode for tracer analysis repeated dilutions of the mother solution were carried out using the model effluent collected from the outlet of the system under analysis. This was to account for the presence of any interfering ions such as NH_4^+.

Figure A6.2 Typical Calibration of the Specific Bromide Ion Electrode

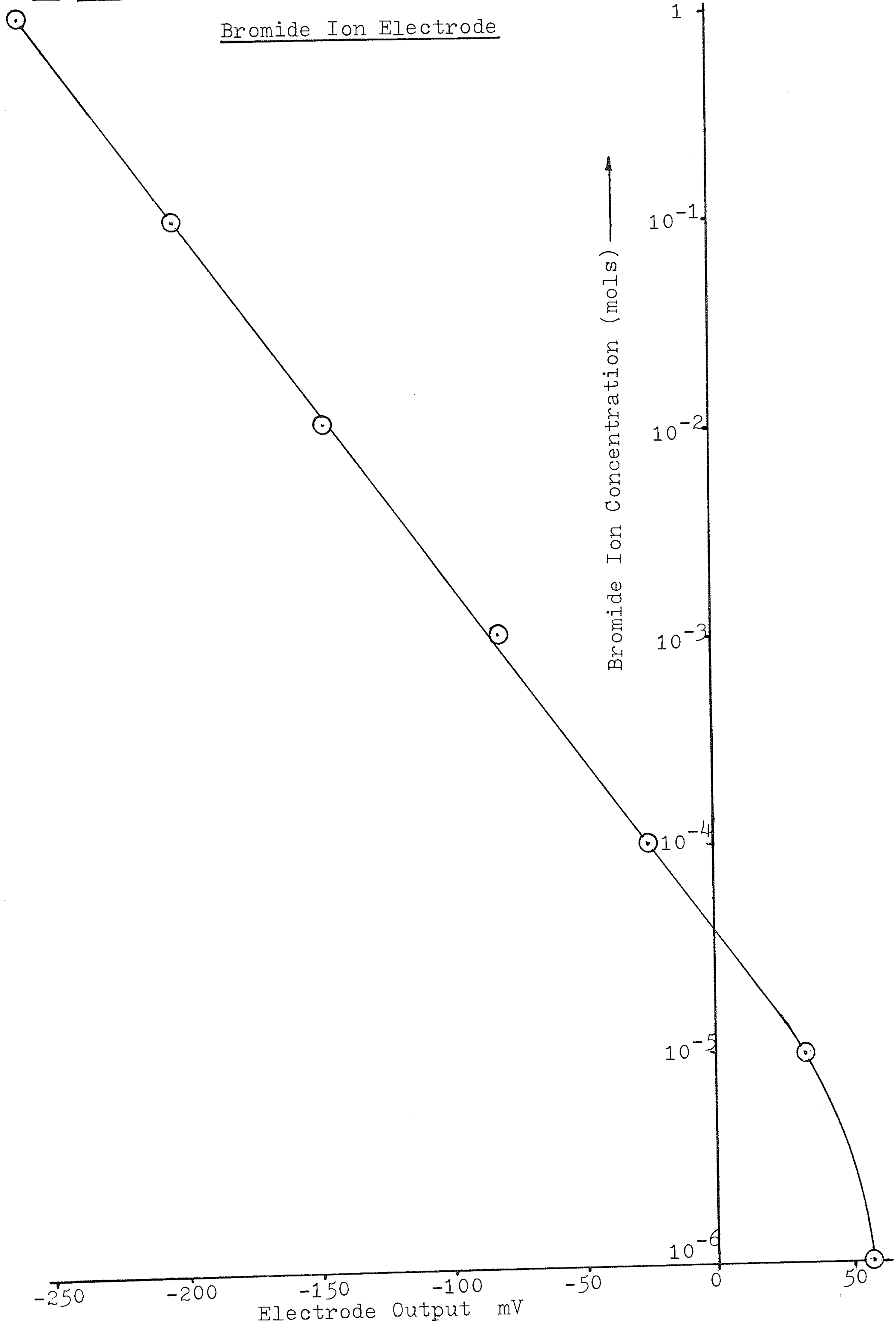

APPENDIX (7)

Nomenclature

A ——— area (L^2)

a ——— hydraulic model parameter given by (v/V) (θ^{-1})

b ——— hydraulic model parameter given by (v^*/V^*) (θ^{-1})

C ——— concentration in general (ML^{-3})

c ——— dimensionless concentration $= C/C_s$

$C(t)$ ——— time-dependent concentration (ML^{-3})

$\bar{C}(t)$ ——— average concentration within a flow system (ML^{-3})

C_A, C_B ——— concentration of A, B (ML^{-3})

C_B^* ——— concentration of B at the penetration depth of A (ML^{-3})

$C_F(t)$ ——— time-dependent concentration of tracer at the system outlet as predicted by the hydraulic models (ML^{-3})

C_{in} ——— inlet concentration (ML^{-3})

$C_N(t)$ ——— time-dependent concentration of tracer in the N th theorètical stirred tank (ML^{-3})

$C_N^*(t)$ ——— time-dependent concentration of tracer in the "dead space" of the hydraulic models (ML^{-3})

C_s ——— concentration at the microbial film surface (ML^{-3})

D ——— diffusivity ($L^2\theta^{-1}$)

D_A, D_B ——— diffusivity of A and B respectively, through microbial film ($L^2\theta^{-1}$)

F ——— microbial film thickness (L)

$\bar{F}$ ——— average microbial film thickness (L)

$\bar{F}_m$ ——— average microbial film thickness as measured $\bar{F}_m = \bar{F} + \delta$ (L)

F_A, F_B ——— thickness of microbial film utilising substrates A and B respectively (L)

F_{crit} ——— critical microbial film thickness, specifies penetration depth of a substrate (L)

F_{crit_A} ——— specifies penetration depth of A (L)

F_{crit_B} ——— specifies penetration depth of B beyond the penetration depth of A (L)

$F_{crit_{in}}, F_{crit_{out}}$ — critical film thickness at the system inlet and outlet respectively (L)

J ——— mass flux $(ML^{-2}\theta^{-1})$

k^* ——— "Monod" rate constant (ML^{-3})

k_o ——— intrinsic zero-order rate constant for substrate utilization $(ML^{-3}\theta^{-1})$

k_{oA} k_{oB} ——— intrinsic rate constants for utilization of A and B respectively $(ML^{-3}\theta^{-1})$

K_B ——— undefined rate constant at a base temperature, T_B

K_T ——— undefined rate constant at a temperature, T

k_t ——— gain constant for relating temperature dependence of K_T

l ——— length, as measured from point of reference (L)

L ——— total length (L)

m_f ——— maintenance energy coefficient for a film culture $(ML^{-3}\theta^{-1})$

m_s ——— specific rate of substrate utilization for maintenance in submerged culture $(L^3\theta^{-1})$

N ——— number of theoretical stirred tanks in a series

N ——— mass flow rate of substrate through microbial film $(M\theta^{-1})$ (used only in Appendix 1)

N_o ——— mass flow rate of substrate into microbial film $(M\theta^{-1})$

$(-r_a)$ ——— bulk rate of substrate utilization, gives rate of substrate removal per unit wetted surface area of microbial film $(ML^{-2}\theta^{-1})$

$(-r_a)_A, (-r_a)_B, (-r_a)_T$ ——— bulk rates of removal of substrates A, B and the total rate of substrate removal in multi-substrate analysis $(ML^{-2}\theta^{-1})$

$(+r_g)$ ——— rate of growth of microbial film $(L\theta^{-1})$

$(-r_v)$ ——— intrinsic rate of substrate removal, gives substrate removal per unit volume of microbial film ($ML^{-3}\theta^{-1}$)

S ——— microbial film exponential growth rate constant (θ^{-1})

S_m ——— microbial film exponential growth rate constant as evaluated from two consecutive film thickness measurements (θ^{-1})

t ——— time (θ)

T ——— duration of tracer experiment (θ), used only in Appendix 2

T ——— temperature

T_B ——— base or datum temperature

u ——— volumetric flow rate ($L^3\theta^{-1}$)

u^* ——— hypothetical flow rate of tracer solution into a "dead space" ($L^3\theta^{-1}$)

V^* ——— volume of the "dead space" in the hydraulic models (L^3)

V_T ——— total volume of liquid retained within a system (L^3)

W ——— inclined plane width (L)

W_d ——— microbial film dry weight/wet weight

X ——— concentration of microbial cells in submerged culture (ML^{-3})

x ——— dimensionless length $= l/L$

Y_{dm} ——— coefficient for microbial dry mass yielded from a unit mass of substrate

Y_{vm} ——— coefficient for volume of microbial film yielded from a unit mass of substrate (L^3M^{-1})

Y_g ——— yield coefficient of substrate used for growth only (unspecified character)

Y_o ——— overall yield coefficient, considers maintenance requirement (unspecified character)

β ——— dimensionless length given by the ratio of substrate penetration depth and microbial film thickness

δ ——— liquid film thickness (L)

σ ———— dimensionless group expressing the ratios of diffusivities and rate constants in a multi-substrate model

M ———— dimension given to indicate mass

L ———— dimension given to indicate length

θ ———— dimension given to indicate time